

Comparative study for the removal of crystal violet from aqueous solution by natural biomass adsorbents of a pinecone, cypress, and oak: kinetics, thermodynamics, and isotherms

Alaa M. Al-Ma'abreh*, Razan Ataallah Abuassaf, Dareen A. Hmedat, Manal AlKhabbas, Samer Alawaideh, Gada Edris

Department of Chemistry, College of Science, Isra University, Amman, Jordan, Tel. +962-799011634; emails: alaa.almaabreh@iu.edu.jo/alaaamabreh@yahoo.com (A.M. Al-Ma'abreh), razan.abuassaf@iu.edu.jo (R.A. Abuassaf), Dareenhmedat@yahoo.com (D.A. Hmedat), Manal.khabbas@iu.edu.jo (M. AlKhabbas), Samerawaideh@yahoo.com (S. Alawaideh), Gadaedris@yahoo.com (G. Edris)

Received 3 May 2022; Accepted 26 August 2022

ABSTRACT

In this study, natural and available biomass of a raw pinecone (P), cypress fruit (C), and oak cupule (O) powders were used as adsorbents for the removal of crystal violet (CV) from aqueous solution. Techniques of FT-IR, SEM, and XRD were employed for the characterization of biomass materials before (P, C, and O) and after adsorption (PCV, CCV, and OCV). Results show that the adsorption capacity of CV is influenced by parameters of dosage, particle size, initial concentration, contact time, pH, and temperature. The best uptake of CV ranged between 80.64 and 105.24 mg/g by P, C, and O under optimal conditions of: 0.07 g O, and 0.05 g P and C, 60 mg/L initial concentration of CV, 80 min. Contact time for O, and 100 min. for C and O, pH 7.0 for P, and pH 9.0 for C and O. The fit to the pseudo-second-order kinetics model suggests chemical adsorption onto P adsorbent. While the fit to pseudo-first-order kinetic model suggests physical adsorption onto C and O adsorbents. The Langmuir isotherm model fitted the experimental data with a maximum adsorption capacity of 80.84, 105.24, and 90.91 mg/g by P, C, and O, respectively. The study revealed that low-cost and eco-friendly biomasses of P, C, and O posed a very good potential as adsorbents for CV dye removal.

Keywords: Adsorption; Crystal violet (CV); Natural biomass; Pinecone; Oak; Cypress

1. Introduction

Recently, environmental pollution caused by hazardous materials has become an alarming concern worldwide. Many recent studies have focused on the effective removal of such pollutants to reduce the risk they pose to living organisms [1]. Different types of organic pollutants have been reported in different water resources. Among these pollutants are organic dyes broadly utilized to pigments products in industries such as textiles, cosmetics, pharmaceuticals, polymers, food, paper, etc. [2]. These dyes do not

undergo natural degradation, so their persistence in aquatic systems hinders the passage of light into the water and disturbs ecosystems by limiting photosynthesis in aquatic plants [3]. For example, released dyes in water streams constitute a risk of eco-toxicity and the potential danger of bio-accumulation. Transport of such contaminants via the food chain could even impact human health [4]. Organic dyes enter the aquatic systems from the outflowing of the paint industry, textile industry, medical industry, and biotechnology industry. CV dye [Fig. 1] is cationic triphenylmethane, which is well-known to be unsafe, mutagenic, carcinogenic,

* Corresponding author.

teratogenic, and mitotic poisoning for living organisms. Despite that, it is continually produced and consumed commercially [5] CV is widely utilized in the textile industry for dyeing cotton, wool, silk, and nylon [6]. Numerous techniques were utilized for the removal of organic and inorganic pollutants, such techniques include chemical precipitation, membrane filtration, ion exchange, electrolysis, coagulation, solvent extraction, reverse osmosis, and electrocoagulation [7]. Most of the common techniques suffer some blemish such as imperfect removal of contaminants, low selectivity, chemical and energy requirements, and high cost [8]. Among various techniques, the adsorption process by solid adsorbents is accepted in environmental treatment applications throughout the world [9] due to its high effectiveness, complete removal of metal ions even at low concentrations, low health risk, ease of operation, environment-friendliness, non-destructiveness, low cost, and ease of adaptation and sorbent material separation from the aqueous phase after finishing treatment [10]. Several studies were conducted in an attempt to remove pollutants from water by utilizing adsorption by natural surfaces.

Various studies have been carried out for the uptake of crystal violet dye from aqueous solutions based on the use of raw natural materials without any treatment. A study showed that tea dust (TD) biomass is utilized as an efficacious and low-cost adsorbent for the uptake of CV dye from industrial wastewater. The batch adsorption technique proceeded under different physicochemical parameters such as adsorbent dosage, pH, initial concentration, and contact time [11]. In another study of the uptake of CV dye by natural clay from the Agadir region, results showed that it was highly affected by the pH, initial dye concentration, and temperature. The maximum adsorption capacity for CV dye was reported to be 264.54 mg/g in the existence of methylene blue and Congo red dyes. It was found that the adsorption of CV dye onto natural clay is better described by the pseudo-second-order model and followed the Langmuir model. Thermodynamic studies confirm that the adsorption process in this study is spontaneous, physical, and endothermic [12]. Lairini et al. [13] succeed to utilize the potato peel as an efficacious agricultural by-product adsorbent for the uptake of CV dye from an aqueous solution without any modification. The maximum uptake efficacy was reported at the optimum contact

time of 20 min, adsorbent dose of 0.5 g/L, initial dye concentration of 20 mg/L, and pH of 6. Equilibrium adsorption data were fitted to follow the Langmuir isotherm model, and the kinetic analysis revealed that adsorption data were fitted with a pseudo-second-order model. Pang et al. [14] employed biomass from pecan nutshell (PN), para chestnut husk (PCH), araucaria bark (AB), and palm cactus (PC) to study the adsorption mechanism of a relevant textile pollutant, CV. The calculation of the adsorption energy on these four biomasses suggested that this dye adsorption process was endothermic and controlled by physical interactions. Successful removal of methylene blue (MB) and CV dyes onto local soil clay was reported. The maximum removal of MB and CV up to 47.82 and 35.71 mg/g, respectively, was achieved by dye molecule adsorption onto soil clay [15]. Results revealed that the unmodified raw dried bark powder of mangrove species *Rhizophora mucronata* is effective for the uptake of CV dye from industrial effluents with 99.8% efficacy. The uptake of CV dye is inversely proportional to particle size and ionic strength and directly proportional to the adsorbent dose, contact time, and initial dye concentration [16].

In this study, pinecone (P), cypress fruit (C), and oak cupule (O) from Jordan were employed as low-cost and eco-friendly adsorbents for the removal of CV dye from an aqueous solution. Effective parameters such as adsorbent dosage, initial dye concentration, contact time, and pH were investigated. The equilibrium and mechanism of the adsorption process were investigated by conducting kinetic and isothermal studies.

2. Experimental

2.1. Reagents and instruments

CV dye (HPLC grade, 99.9%) was acquired from Sigma Aldrich and used as received without further purification. 1 g was dissolved in 1.0 L of double-distilled water to prepare stock solutions. The required working concentrations of (10–100 mg/L) were prepared from the respective stock solutions. The solution pH was adjusted using 0.1 M HCl and 0.1 M NaOH solutions. FT-IR instrument (SENSOR from BRUKER) was used to detect the functional groups existing on the biomass adsorbent material (P, C, and O) and their significance in the removal process. The agricultural adsorbents spectra fell within the wavenumber region of 500–4,000 cm^{-1} . Scanning electron microscopy (SEM; Model: A Phenom XL G2 scanning electron microscope from Thermo Fisher Scientific) was used to obtain images of adsorbent materials. X-ray diffraction (XRD) analyses were carried out in PANalytical B. V. Lelyweg 17602 EA ALMELO-Netherlands instrument.

2.2. Preparation of adsorbent

Both pinecone and cypress fruit adsorbents were collected from local pine trees (Isra University Campus-Jordan), while the oak cupule was collected from Jerash province – Jordan. Firstly, the impurities were rinsed with distilled water from the three materials. Then samples were dried in an oven at 70°C for 48 h. The dried samples were

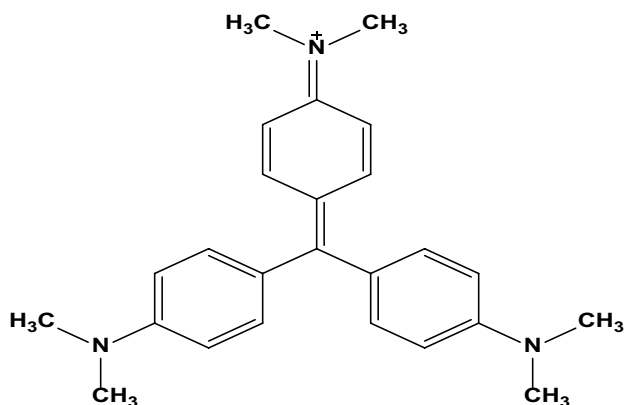


Fig. 1. Crystal violet dye $\text{C}_{25}\text{N}_3\text{H}_{30}\text{Cl}$.

blended using a food processor and then ground to obtain a fine powder. Finally, the powder of each material was sieved to particle sizes of 125–180, 180–250, and 250–350 μm. The powdered adsorbent of the three materials (P, C, and O) was stored and used without any pretreatment for removing CV dye.

2.3. Characterization of adsorbents

The surface morphology of raw P, C, and O powders was established through scanning electron microscopy (SEM, Model: A Phenom XL G2 scanning electron microscope from Thermo-Fisher Scientific), Fourier transform infrared (A Tensor FTIR Bruker), and X-ray photoelectron spectroscopy. A thermo pH-meter was used for pH measurements.

2.4. Batch adsorption experiment

The influence of all examined parameters was analyzed using batch adsorption experiments. A 50 mL of CV solution at different concentrations was conveyed into a conical flask containing a measured mass of adsorbent. The flask contents were shaken for a specific time with a speed of 120 rpm. Then the solution was filtered off using a Nylon filter membrane. The filtrate was then subjected to absorbance measurements for concentration determination. The effects of contact time (20–140 min), adsorbent particle size (125, 180, and 250 μm), initial CV concentration (10–70 mg/L), adsorbent (P, C, and O) dose (0.01–0.09 g), and solution pH 5–11 were studied. A UV-6100 PC double beam spectrophotometer was used to determine the concentrations of CV in the supernatant solutions at a wavelength of 580 nm. The amount of CV dye adsorbed onto the adsorbent, q_e (mg/g), was computed using the following material balance relationship [17]:

$$q_e = \frac{(C_i - C_{eq})V}{m} \quad (1)$$

where q_e (mg/g) is the equilibrium quantity of the adsorbed moiety; C_i (mg/L) is the initial concentration of the adsorbate; C_{eq} (mg/L) are the equilibrium concentration of the adsorbate; V (L) is the volume of solution.

Kinetic studies were performed to determine the adsorption rate of CV onto adsorbents of P, C, and O in individually. Langmuir and Freundlich model isotherms were employed to understand the mechanism of CV adsorption onto the adsorbent materials. The adsorption capacity was determined using the following equations:

$$\text{Mass of CV absorbed} = (C_i - C_f) \times V \quad (2)$$

$$\text{Adsorption capacity} = \frac{M_{\text{adsorbate}}}{M_{\text{adsorbent}}} \quad (3)$$

where C_i is the initial concentration of adsorbate in (mg/L); C_f is the final concentration of adsorbate in (mg/L); V is

the volume of the solution in (L); $M_{\text{adsorbate}}$ is the mass of adsorbate in (g); $M_{\text{adsorbent}}$ is the mass of adsorbent in (g).

The rate of CV adsorption was modeled using pseudo-first-order and pseudo-second-order kinetics. The linearized pseudo-first-order kinetic equation proposed by Lagergren was used [18]:

$$\log(q_e - q_t) = \log(q_e) - \left(\frac{k_1}{2.303}\right)t \quad (4)$$

where k_1 is the rate constant of the pseudo-first-order (min^{-1}), q_e is the equilibrium amount of adsorbed material in (mg/g), q_t is the equilibrium amount of adsorbed material at time t (mg/g),

The linearized pseudo-second-order model used is:

$$\frac{t}{q_t} = \frac{1}{k_2 q_e^2} - \frac{1}{q_e} t \quad (5)$$

where k_2 is the rate constant of the pseudo-second-order (g/mg·min), q_e is the equilibrium amount of adsorbed material in (mg/g), and q_t is the equilibrium amount of adsorbed material in at time t (mg/g).

The value of k_2 was calculated from the plot of t/q_t vs. t where $(1/k_2 q_e^2)$ was the intercept and $1/q_e$ was the slope of the plot.

The linearized Langmuir isotherm model used was expressed by the following equation [19]:

$$\frac{C_e}{q_e} = \frac{1}{K_L q_m} + \frac{C_e}{q_m} \quad (6)$$

where q_e is the equilibrium amount of the adsorbed material (mg/g), q_m is the maximum adsorption capacity (mg/g), K_L is the Langmuir isotherm constant related to the adsorption energy, C_e is the equilibrium (final) concentration of adsorbate in the solution (mg/L).

K_L and q_m were calculated from the linear plot of C_e/q_e vs C_e where $(1/q_m)$ was the slope of the straight line, and $1/(K_L q_m)$ was the y -intercept. K_L (i.e., also known as association constant expressed in L/mg) was used to determine the affinity of the adsorbate to the surface of the adsorbent. The dimensionless parameter R_L was calculated using Eq. (7). This parameter can be used to predict the adsorption efficacy of the adsorbent. The process is irreversible if $R_L = 0$, favourable if $R_L < 1$, linear if $R_L = 1$ and unfavourable if $R_L > 1$:

$$R_L = \frac{1}{1 + K_L C_i} \quad (7)$$

where K_L is the Langmuir isotherm constant determined in Eq. (6), C_i is the initial concentration of the adsorbate.

The equation used for Freundlich isotherm model was as follows:

$$\log q_e = \log K_f + \frac{1}{n} \log C_e \quad (8)$$

where q_e is the equilibrium amount of adsorbate in (mg/g), C_e is the equilibrium concentration of adsorbate in (mg/L), K_f is the Freundlich isotherm constant (mg/g), and n is the adsorption intensity.

The values of K_f and n were investigated from the y -intercept and the slope of the plot ($\log q_e$ vs $\log C_e$).

The rate-limiting step for the adsorption of CV onto P, C, and O adsorbent materials was investigated using the intraparticle model according to the following equation:

$$q_t = K_{id} t^{1/2} = C \quad (9)$$

where q_t is the amount of adsorbed CV (mg/g), K_{id} is the rate constant for intraparticle diffusion ($\text{mg/g}\cdot\text{min}^{0.5}$), and $t^{1/2}$ is the square root of time ($\text{min}^{0.5}$).

Thermodynamic experiments were performed under the same experimental conditions previously applied in the adsorption equilibrium; thus, under temperature variation (30°C, 40°C, and 50°C) and constant agitation of 120 rpm. It was possible to calculate fundamental thermodynamic state functions of the adsorption (enthalpy, ΔH° , and entropy, ΔS°) from Van't Hoff's equation:

$$\text{Hoff's equation: } \ln(K_L) = \frac{\Delta S^\circ}{R} - \frac{\Delta H^\circ}{T} \left(\frac{1}{T} \right) \quad (10)$$

Gibbs free energy (ΔG°) can be calculated by:

$$\Delta G^\circ = -RT \ln(K_L) \quad (11)$$

where T is the temperature at which the adsorption takes place in Kelvin (K), K_L is the adsorption equilibrium constant according to the best-fitted model, obtained at each temperature, which is dimensionless, R is the universal constant of ideal gases, 8.314 J/K·mol.

3. Results and discussion

3.1. Characterization of adsorbent

The three adsorbents (P, C, and O) were characterized using FTIR, SEM, and XRD analyses.

3.1.1. FTIR analysis

FT-IR analysis of P, C, and O adsorbents revealed the existence of different functional groups like aldehydes, alcohols, carboxylic, etc. Such groups serve as active sites for adsorption. Fig. 2a and b show that many bands for functional groups such as peaks at 3,331.13; 2,935; 1,619.5; (1,370 and 1,224), 1,023.78; and 552.03–1,023.78 cm^{-1} which

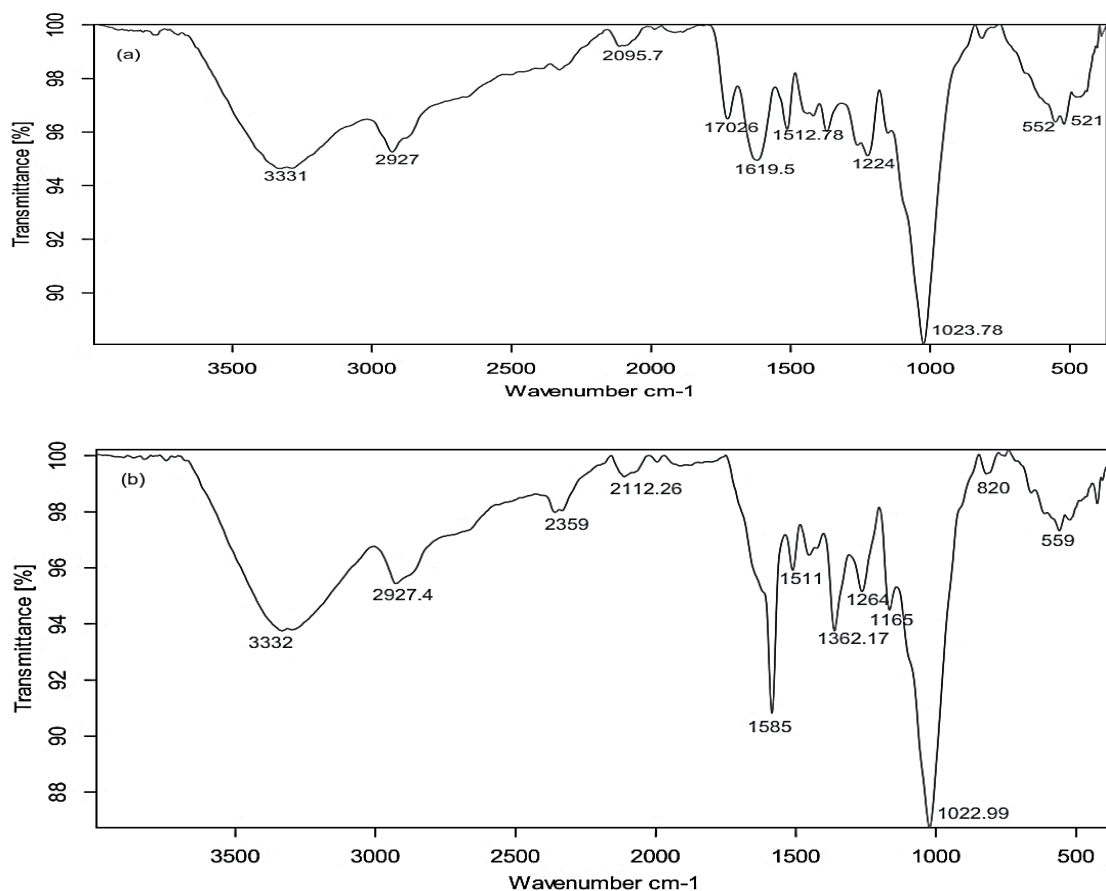


Fig. 2. FT-IR analysis of raw pinecone powder (a) before adsorption P and (b) after adsorption PCV.

are assigned to the stretching vibration for bonds of O–H, (–CH₃ and –CH₂), C=O for carboxyl, –OH for phenol, C–O for 1° alcohol, and –C–N– and –C–C–, respectively [20,21]. By comparing Fig. 2a and b, the obvious shifts in peaks and changes in intensity confirm the adsorption of CV dye onto the P.

Table 1 summarizes FT-IR analysis results for samples of P, C, O, PCV, CCV, and OCV.

Fig. 3a and b represent FT-IR spectra of C adsorbent and C after adsorption of the dye (CCV).

Fig. 4a and b represent the FT-IR spectra of O adsorbent and O after adsorption of the dye (OCV).

3.1.2. SEM analysis of adsorbent material

The adsorbents are powder and have a brown color with different shades. The surface morphology of adsorbents was investigated by scanning electron microscope. Fig. 5a–f show the SEM images of the surface of P, C, and O adsorbents prior to and after the adsorption of CV dye. The remarkable difference between the images before and after the adsorption process through the appearance of aggregates in Fig. 5b, d, and f confirm the occurrence of adsorption.

3.1.3. XRD analysis of adsorbent material

XRD was used to determine the crystallographic structure of all materials in the study. The obtained spectra are depicted in Fig. 6. By compared spectra before and after adsorption, there are changes in intensity and peak broadening.

3.2. Batch adsorption of crystal violet

3.2.1. Influence of adsorbent dosage

The effect of adsorbent dosage was investigated by computing the removal efficacy and the adsorption capacity of CV dye onto P, C, and O, separately. The dose of adsorbents varied from 0.01 to 0.09 g using seven doses. The batch adsorptions experiments were conducted keeping the contact time at 1.0 h, and the initial concentration at 20 mg/L, the temperature at 30°C, and the pH at 7. From the results shown in Fig. 7a–c, it is evident that the adsorption capacity decreased (from 60.26 to 10.09 mg/g) with the increasing adsorbent dose for P, (from 60.72 to 9.69 mg/g) for C, and (from 80.99 to 9.49) for O. A dose of 0.07 for O and 0.05 for P and C were selected for further investigations as optimal dose. The adsorption behavior is elucidated based on the existence of fixed moieties of CV vs. more abundant binding sites with rising the dose.

3.2.2. Influence of contact time

Contact time is one of the factors that greatly influenced the efficacy of the adsorption process. The contact time varied from 20 to 140 min. The batch adsorptions experiments were conducted under conditions of 0.07 g of O and 0.05 g of P and C adsorbents, 7.0 pH, 120-rpm shaking speed, and a temperature of 30°C ± 1°C. The results regarding the removal of CV by utilized adsorbents are presented in Fig. 8. For the investigated adsorbent the adsorption capacity increased rapidly at the first stages under the proposed conditions as shown in Fig. 8. The initial adsorption stage is rapid due to the number of available sites. Equilibrium was

Table 1
FTIR results

	Raw (P) powder (cm ⁻¹)	CV adsorbed on P (PCV) (cm ⁻¹)	Raw (C) powder (cm ⁻¹)	CV adsorbed on C (CCV) (cm ⁻¹)	Raw (O) powder (cm ⁻¹)	CV adsorbed on O (OCV) (cm ⁻¹)
O–H stretching vibration	3,331.13	3,332	3,278.96	3,289.47	3,332.56	3,335.43
Aliphatic C–H group stretching vibra- tions of the –CH ₃ and –CH ₂ groups	2,935	2,927.4	2,933.36	2,926.17	2,925.52	2,918.36
Stretching vibration of C=O of carboxylic groups	1,619.5	1,585	1,738.41	1,685.08	1,603.04	1,584.81
Carboxylic/aromatic hydroxyl (–OH) stretching of phenol group	1,370 and 1,224	1,362.17 and 1,264	1,367.84 and 1,219.85	1,442.44 and 1,267.04	1,435.58 and 1,367.84	1,361.20 and 1,167.72
Stretching vibration of C–O of the pri- mary alcohol group	1,023.78	1,022.99	1,021.82	1,021.78	1,021.78	1,024.49
–C–N– stretching and –C–C– stretching	552.03–1,023.78	559–820	524.63–1,021.82	557.76–1,021.78	525.69–1,021.78	563.69–1,024.49

CV: Crystal violet; P: Pinecone; C: Cypress fruit; O: Oak cupule.

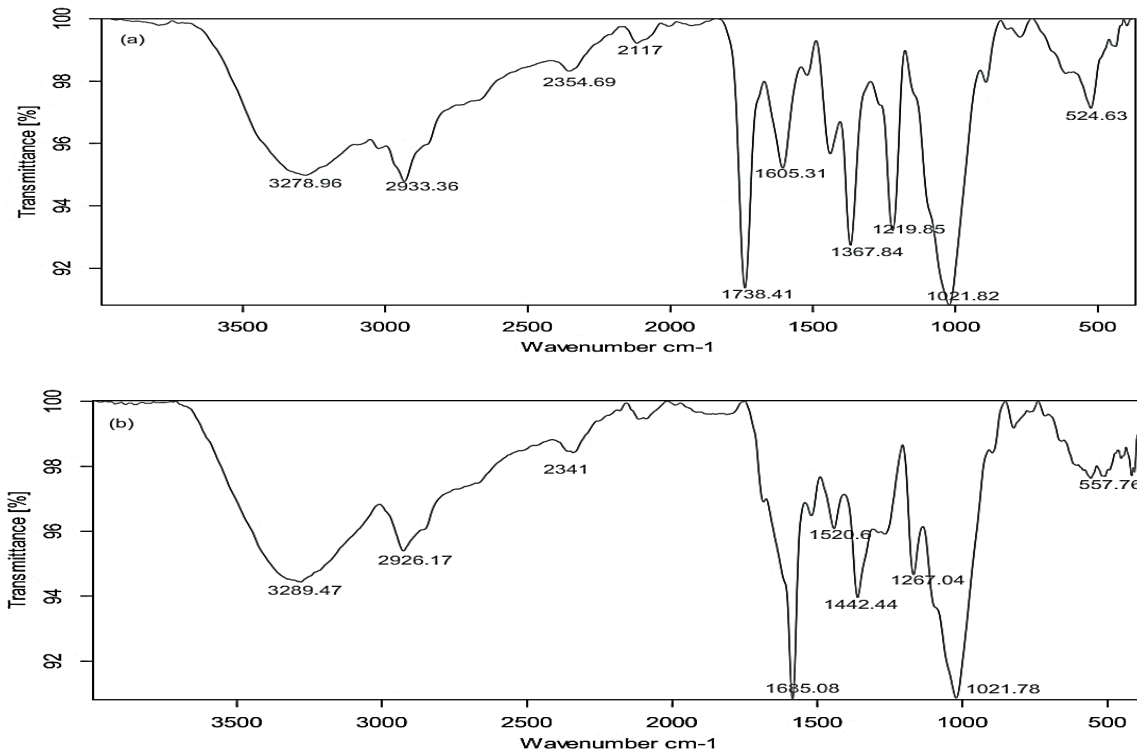


Fig. 3. FT-IR analysis of raw cypress fruit powder (a) before adsorption C and (b) after adsorption CCV.

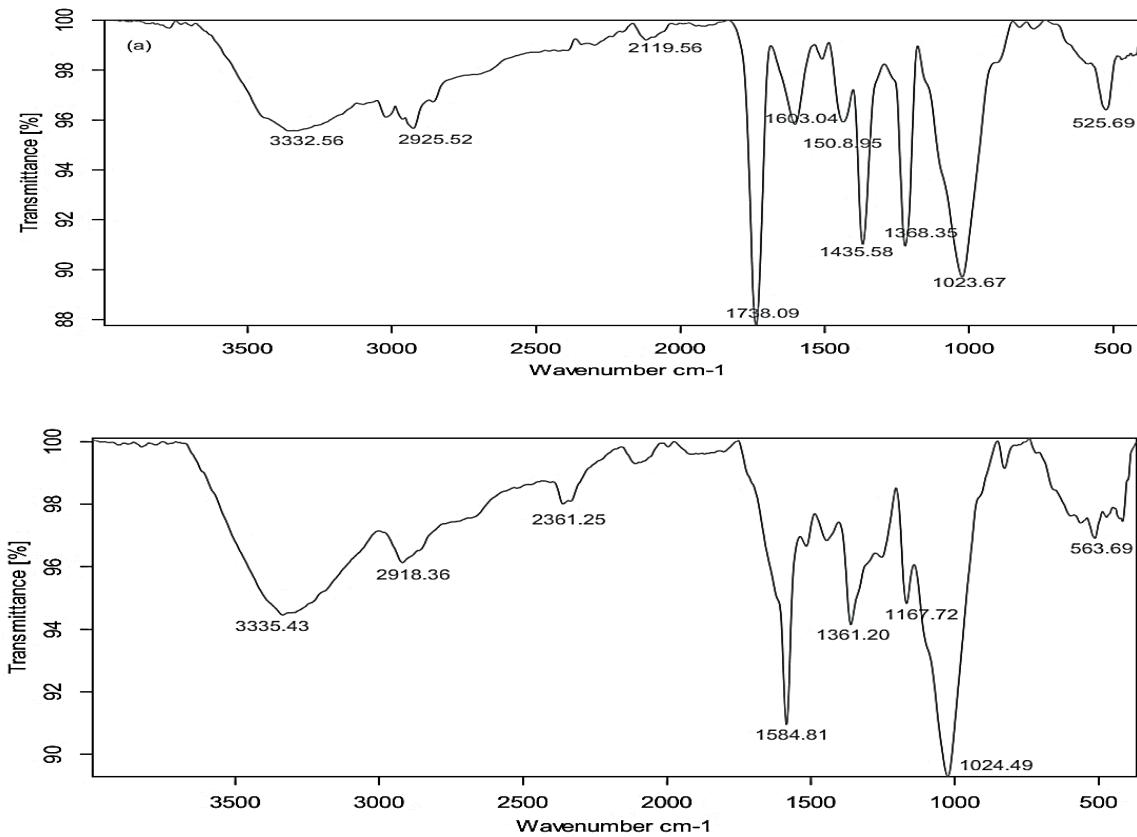


Fig. 4. FT-IR analysis of raw oak cupule powder (a) before adsorption O and (b) after adsorption OCV.

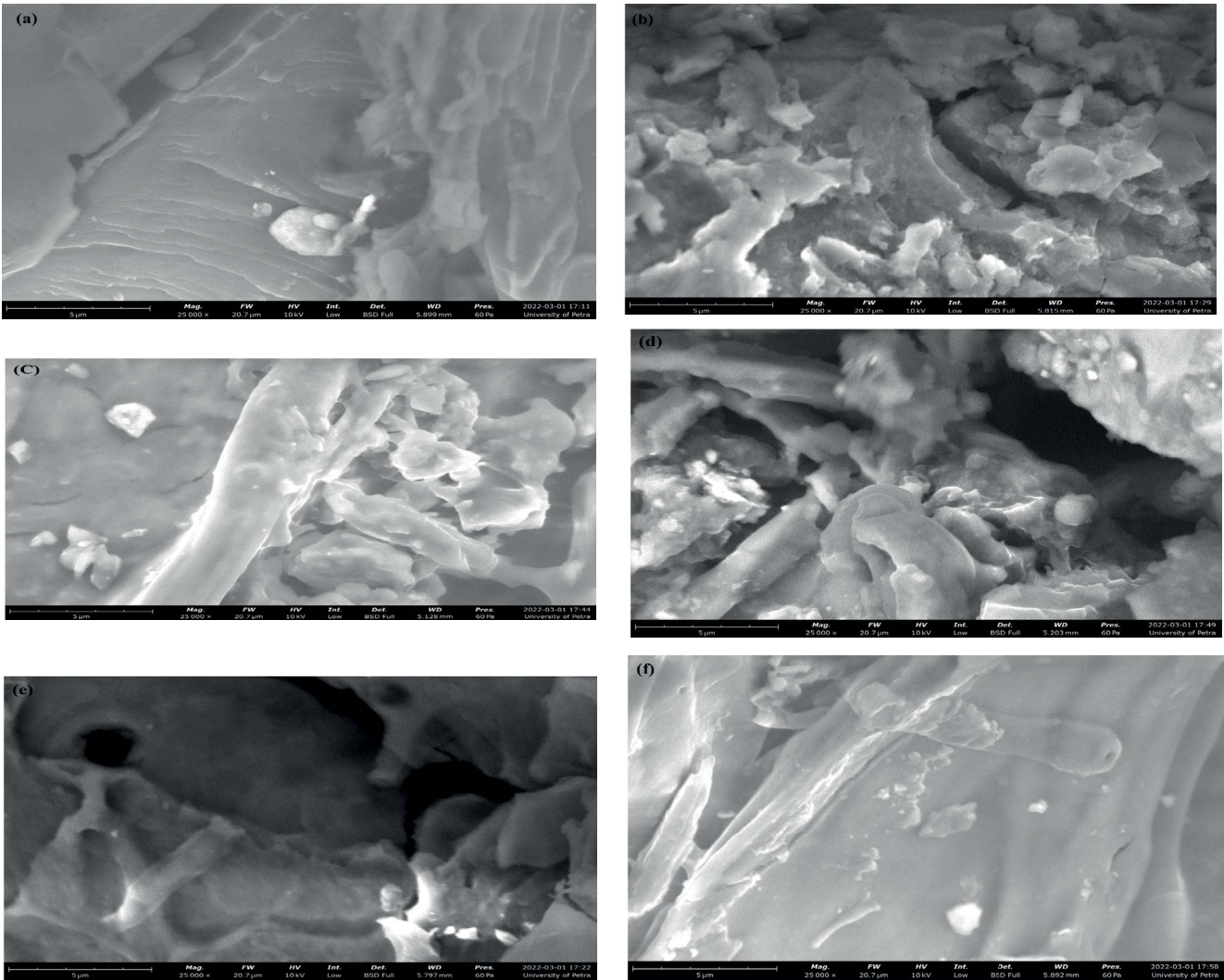
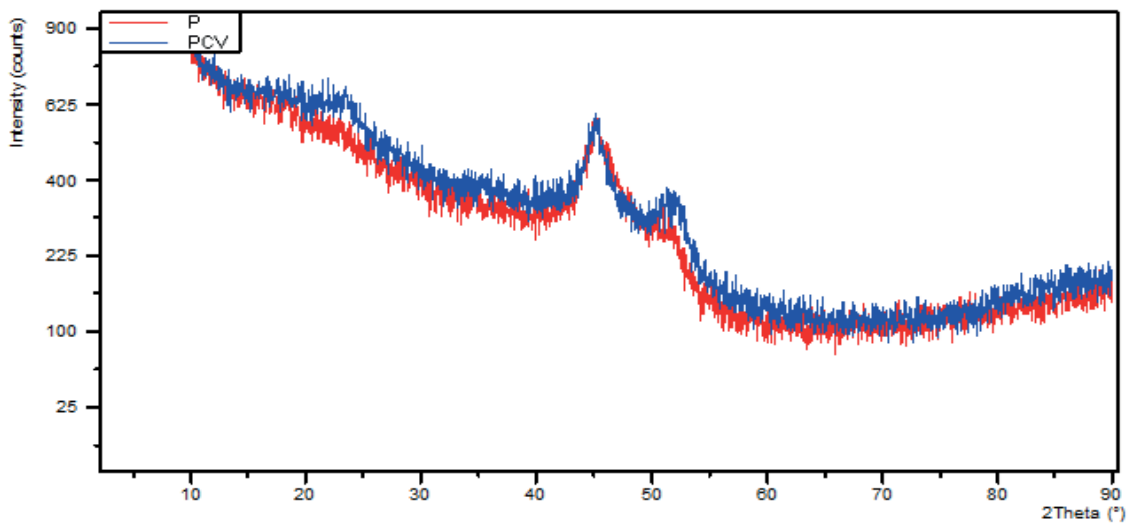


Fig. 5. SEM analysis of (a) pinecone biomass before adsorption, (b) pinecone biomass after, (c) cypress fruit biomass before adsorption, (d) cypress fruit biomass after adsorption, (e) oak cupule biomass before adsorption, and (f) oak cupule biomass before adsorption.



(Continued)

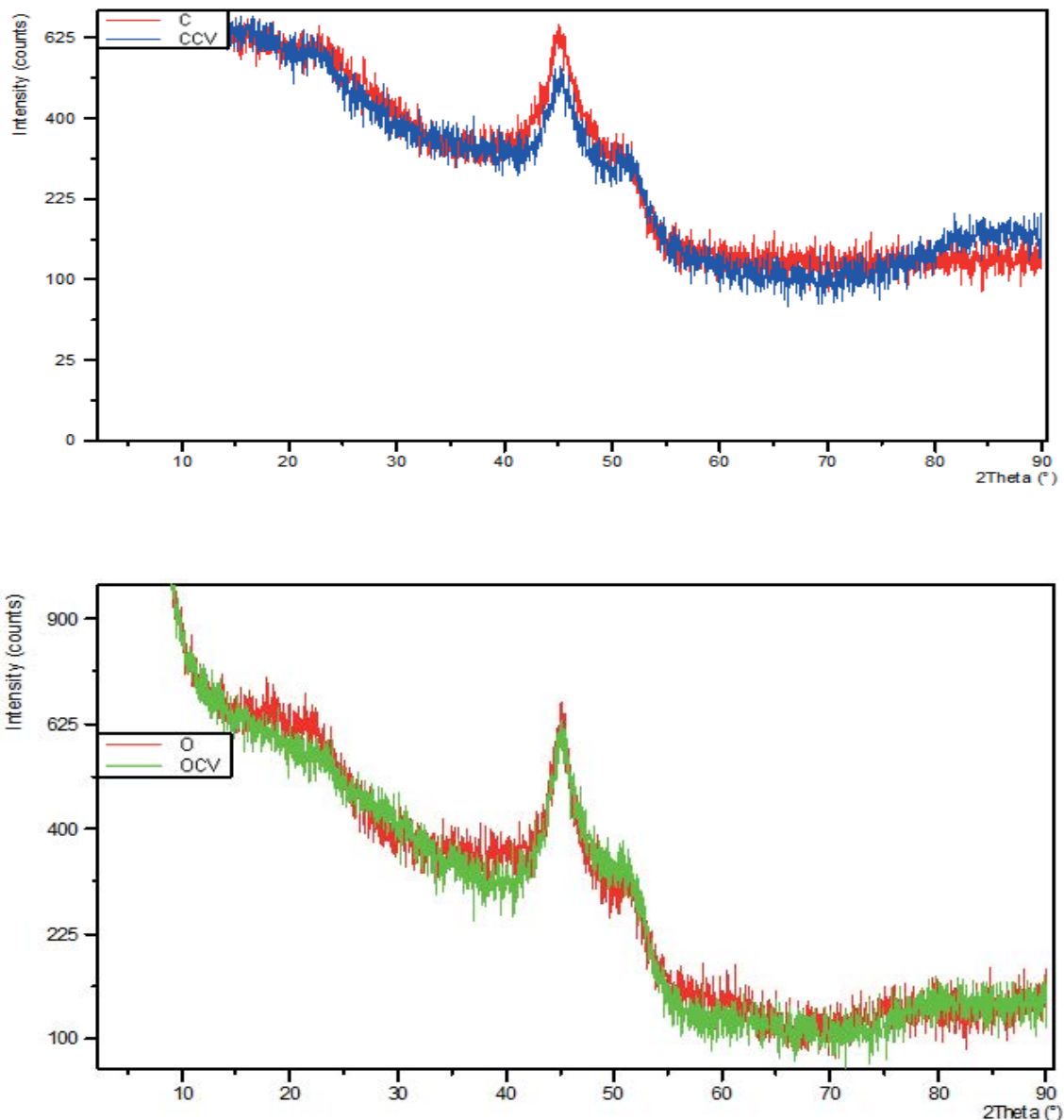


Fig. 6. XRD analysis of (a) pinecone biomass before adsorption-p- and after adsorption-PCV-, (b) cypress fruit biomass before adsorption-C- and cypress fruit biomass after adsorption-CCV-, and (c) oak cupule biomass before adsorption-O- and oak cupule biomass after adsorption-OCV-.

touched after 80 min for O (44.27 mg/g) and 100 min for P (44.1 mg/g) and C (48.09 mg/g).

3.2.3. Influence of adsorbate initial concentration

The influence of the initial concentration of CV dye on the adsorption capacity of P, C, and O adsorbents was investigated at a concentration range of 10–70 mg/L (Fig. 9). At the initial stages the adsorption capacity of P, C, and O increased rapidly with the rises in CV concentration as Fig. 9 demonstrated. The equilibrium is touched at the concentration of 60 mg/L for all used adsorbents (P, C, and O). The adsorption capacity increases due to the enhancement of

diffusion rate toward the active sites, by rising CV concentration [22,23]. At the equilibrium, the active sites on the adsorbent surface become saturated with CV moieties [24,25]. The adsorption capacities at the optimal concentration (60 mg/L) were 115.82, 68.4, and 72.7 for P, C, and O, respectively.

3.2.4. Influence of pH

The influence of pH on the adsorption of CV dye onto P, C, and O was investigated at a temperature of $30^{\circ}\text{C} \pm 1^{\circ}\text{C}$, and the investigated optimal conditions of adsorbent dose, CV concentration, and contact time. The batch adsorption

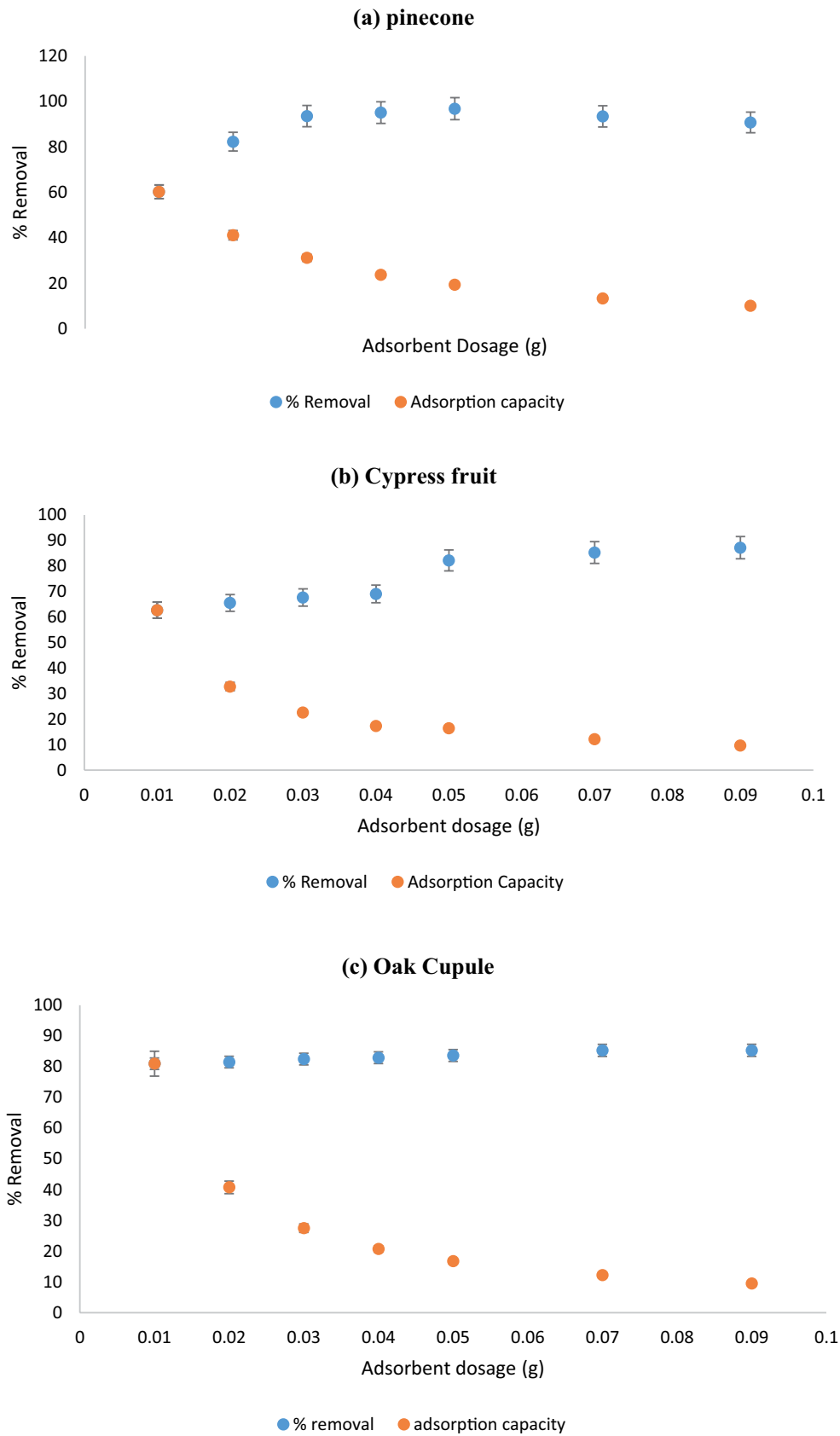


Fig. 7. Influence of adsorbent dosage on the adsorption of crystal violet dye, [Experimental conditions: dosage = 0.01–0.09 g, $C_i = 20$ mg/L; pH = 7.0; contact time = 60 min; $T = 30^\circ\text{C} \pm 1^\circ\text{C}$] onto (a) pinecone, (b) cypress fruit, and (c) oak cupule.

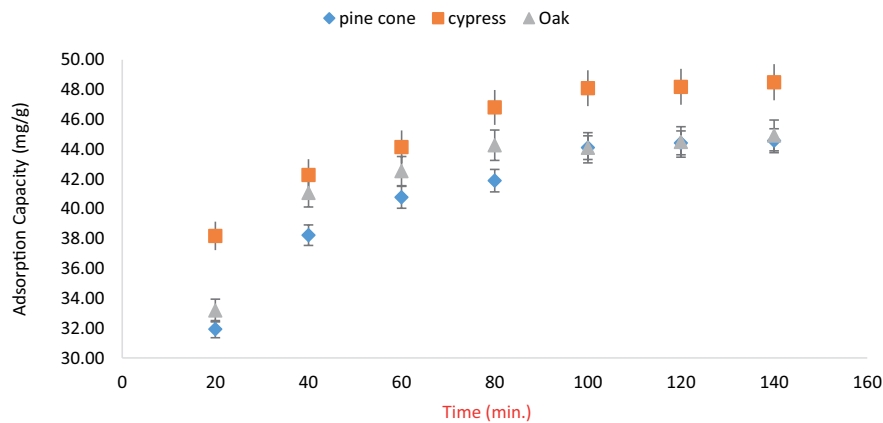


Fig. 8. Influence of contact time on the adsorption of CV dye, [Experimental conditions: dose = 0.05 P, 0.05 C, and 0.07 O; contact time = 20–140 min; $C_i = 20$ mg/L; pH = 7.0; $T = 30^\circ\text{C} \pm 1^\circ\text{C}$].

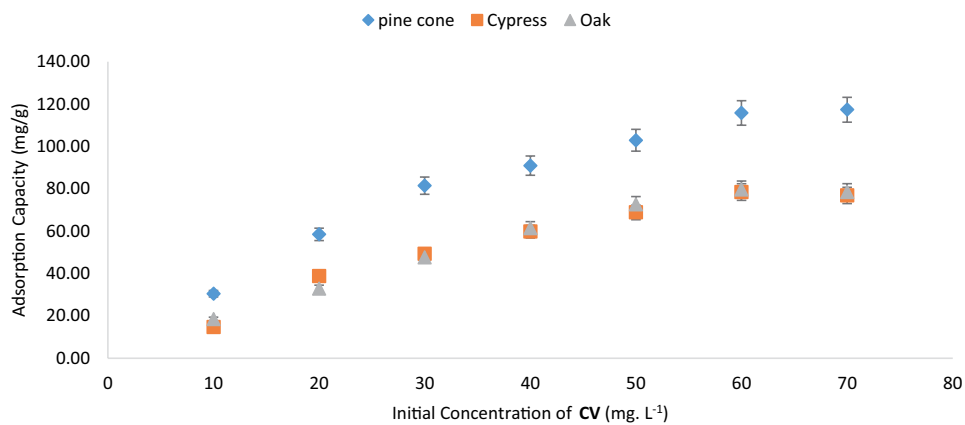


Fig. 9. Influence of adsorbate initial concentration (10–70 mg/L) on the adsorption of CV dye, [Experimental conditions: dose = 0.05 P, 0.05 C, and 0.07 O; contact time = 80 min. For O, and 100 min. For P and C; pH = 7.0; $T = 30^\circ\text{C} \pm 1^\circ\text{C}$].

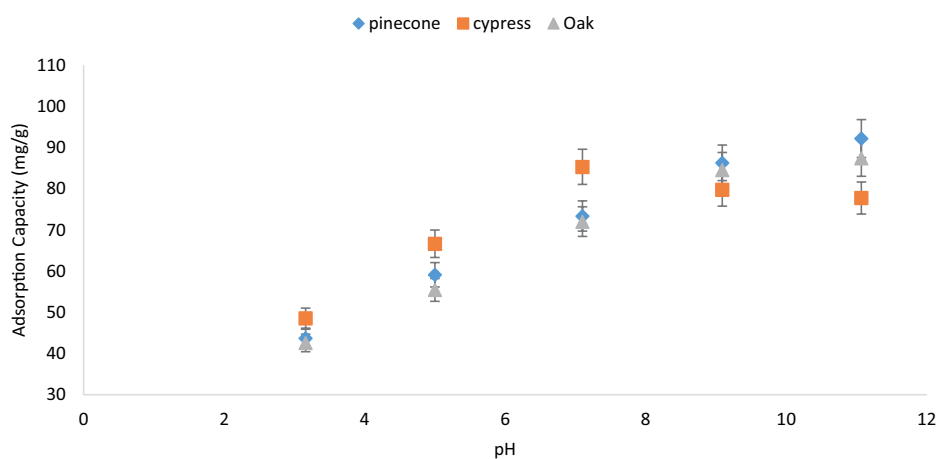


Fig. 10. Influence of pH (3–11) on the adsorption of CV dye on a pinecone, cypress fruit, and oak cupule; [Experimental conditions: dose = 0.05 P, 0.05 C, and 0.07 O; contact time = 80 min. For O, and 100 min. For P and C; $C_i = 60$ mg/L; $T = 30^\circ\text{C} \pm 1^\circ\text{C}$].

experiments were conducted at a pH range between 5 and 11. As Fig. 10 demonstrates, for P and O adsorbents the adsorption capacities were observed to increase obviously with rising pH from 5.0 to 11.0. While for C adsorbent the

adsorption capacity increases to neutral and then falls at a basic solution. The behavior of adsorption process ascribed to the competition of H^+ with CV moieties at low pH (high concentration of H^+ [26]). Further increase in pH caused a

decrease in repulsion between the positively charged CV moieties and the adsorbent [27]. The variation in solution pH influences the surface properties of the adsorbents surfaces [28]. For the C adsorbent, a further increase in pH beyond 7 leads to a decrease in adsorption capacity. Thus, the optimum pH value for CV dye adsorption onto C was found to be 7.0.

pH_{pzc} value has an important role in elaborating adsorption behavior by varying the pH of the solution. pH_{pzc} is the value of pH value at which the net charge on the adsorbent surface is equal to zero. When $pH_{pzc} > pH$ this results in positively charged surface, while negatively charged surface is obtained when $pH_{pzc} < pH$ [29]. A 0.15 g of each P, C, and O were shaken with 50 mL of 0.01 M NaCl solutions for 24 h at six pH values (2, 4, 6, 8, 10, 12) in an attempt to determine the pH_{pzc} values for the three adsorbents. The final pH values were then measured for all solutions. Plots of pH_f vs. pH_i for the three adsorbents were constructed for the determination of pH_{pzc} . It's found that the pH_{pzc} for C adsorbents is equal to 7.0. This elaborates the decreases in adsorption beyond neutrality due to the repulsion between CV and +ve surface of C. For P and O adsorbents, it is remarkable, that the pH_{pzc} value is equal to 9.0 in which the surfaces have -ve charge.

3.2.5. Influence of adsorbent particle size

The batch adsorption experiments were conducted at three values of particle size (125, 180, and 250 μm). The influence of adsorbents particle size on the adsorption of CV was investigated at the assigned optimal conditions for each of P, C, and O. Increasing particle size of adsorbent provides fewer sites on the surface as shown in Fig. 11. Inverse relationship was investigated between removal efficacy and particle size.

3.2.6. Adsorption kinetic studies

Adsorption kinetic studies were carried out for the adsorption of CV onto P, C, and O. The obtained experimental data were tailored to pseudo-first-order, pseudo-second-order, and intraparticle diffusion kinetics models. Rate constants were determined based on the linearized plots presented in Figs. 12–15. Table 2 summarized the obtained results of the conducted kinetic studies. The R^2 value of 0.9889 indicates that CV adsorption onto P is fitted to pseudo-second-order (Fig. 12). In contrast, R^2 values of 0.9904 and 0.9715 for C and O, respectively, indicate the demonstration of pseudo-first-order of CV adsorption (Figs. 13 and 14).

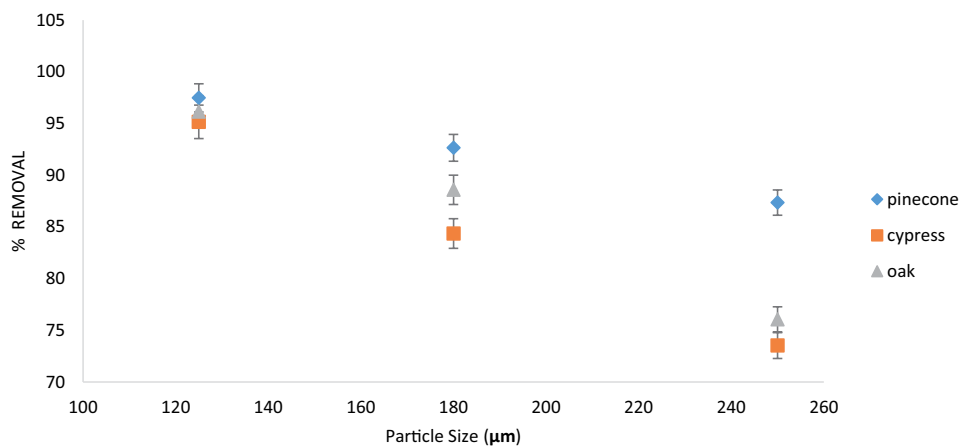


Fig. 11. Influence of adsorbent particle size (125–250 μm) on the adsorption of CV dye, [Experimental conditions: dose = 0.05 P, 0.05 C, and 0.07 O; pH = 7; contact time = 80 min. For O, and 100 min. For P and C; C_i = 60 mg/L; T = 30°C \pm 1°C].

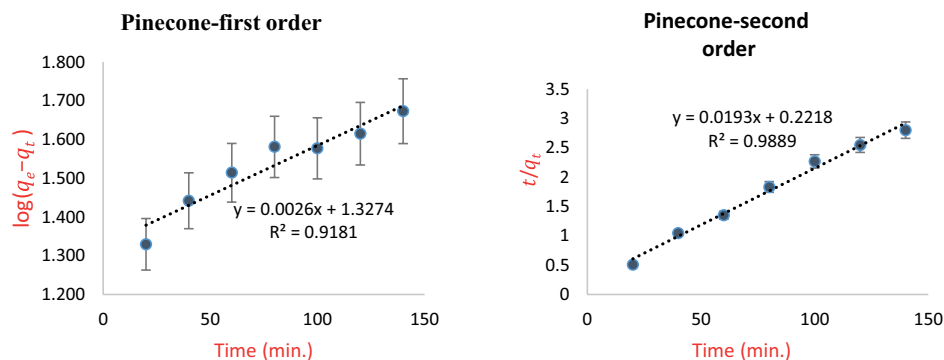


Fig. 12. Kinetic studies of the adsorption of CV dye onto pinecone powder (P), [Experimental conditions: pH = 7.0; C_i = 60 mg/L; time = (20–140 min); dose = 0.05 g; T = 30°C \pm 1°C].

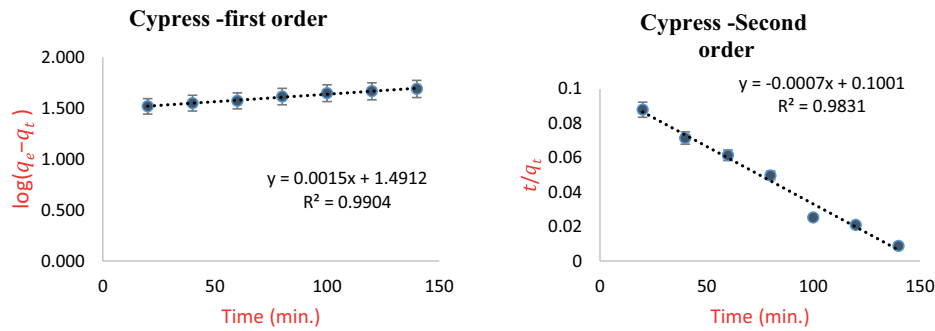


Fig. 13. Kinetic studies of the adsorption of CV dye onto cypress fruit powder (C), [Experimental conditions: pH = 7.0; $C_i = 60$ mg/L; time = (20–140 min); dose = 0.05 g; $T = 30^\circ\text{C} \pm 1^\circ\text{C}$].

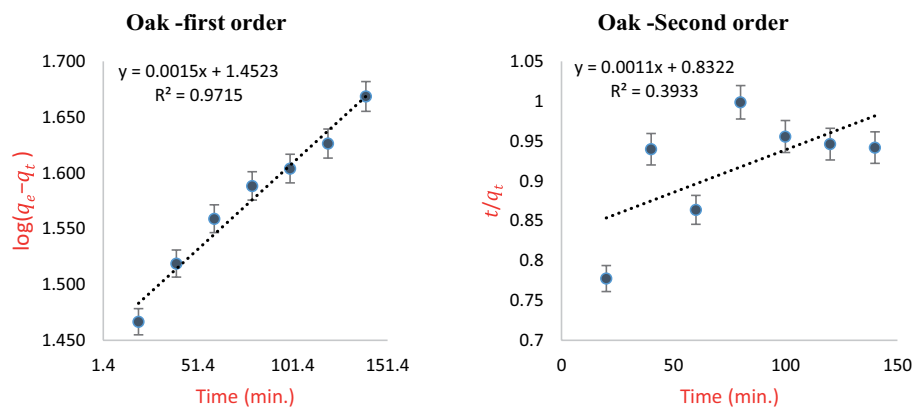


Fig. 14. Kinetic studies of the adsorption of CV dye onto oak cupule powder (O), [Experimental conditions: pH = 7.0; $C_i = 60$ mg/L; time = (20–140 min); dose = 0.07 g; $T = 30^\circ\text{C} \pm 1^\circ\text{C}$].

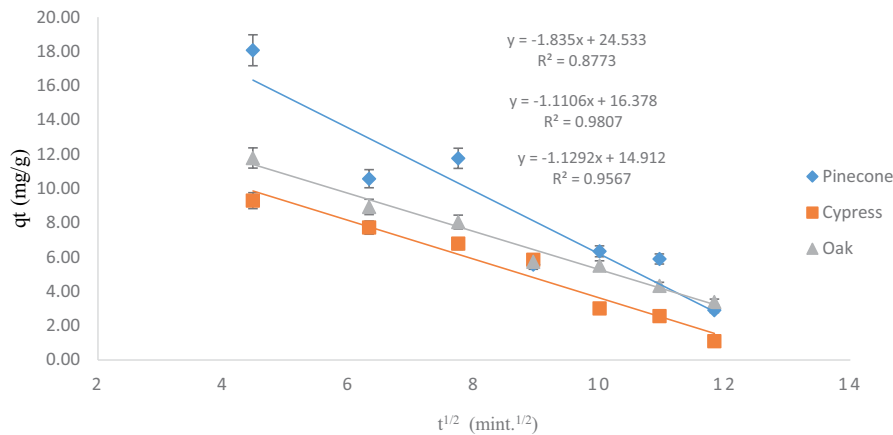


Fig. 15. Intraparticle model for the adsorption of CV onto P, C, and O adsorbent materials.

The intra-particle diffusion model was employed in an attempt to predict the rate-limiting step for the adsorption of CV onto P, C, and O adsorbents. The mechanism of the adsorption process is described by consecutive steps of (i) transport of the adsorbate from the bulk solution to the surface of the adsorbent, (ii) diffusion of adsorbate molecules into the pores of adsorbent if existence, and (iii) adsorption of adsorbate molecules onto the pores interior surface [30]. According to this model if the intercept C is equal to zero then the diffusion will be the sole rate-limiting step.

Surface adsorption will contribute to the mechanism as the C value rises. Fig. 15 elucidates that the intra-particle diffusion is not the rate-limiting step and there is a contribution of surface adsorption hence C is not zero for all adsorbents.

3.2.7. Adsorption isotherms

Langmuir and Freundlich isotherms were used to indicate the mechanisms of adsorption of CV dye onto raw P, C, and O powders. Figs. 16–18 illustrate the application of

Table 2
Kinetics constants

	First-order kinetics		Second-order kinetics		Intraparticle diffusion kinetics	
	R^2	k_1 (min^{-1})	R^2	k_2 ($\text{g}/\text{mg}\cdot\text{min}$)	R^2	K_{id} ($\text{mg}/\text{g}\cdot\text{min}^{0.5}$)
Pinecone	0.9181	2.6×10^{-3}	0.9889	1.93×10^{-2}	0.8773	1.835
Cypress fruit	0.9904	1.5×10^{-3}	0.9831	-7.00×10^{-4}	0.9567	1.1292
Oak cupule	0.9715	1.5×10^{-3}	0.3933	1.1×10^{-3}	0.9807	1.1106

R^2 : Correlation coefficient; k_1 : Rate constant for pseudo-first-order; k_2 : Rate constant for pseudo-second-order.

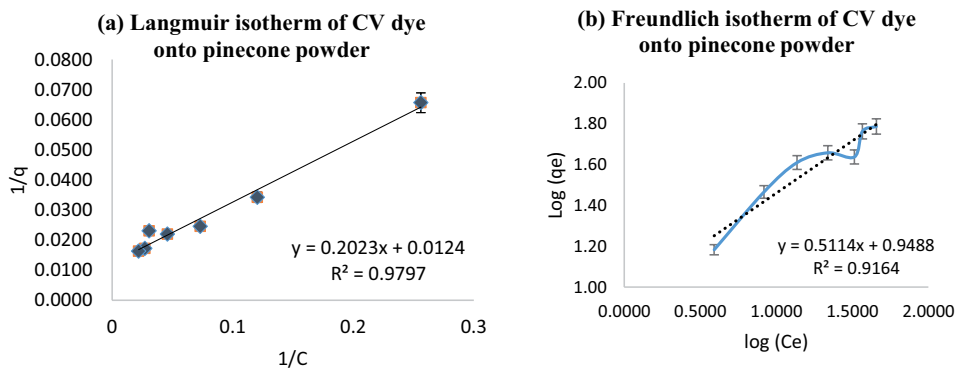


Fig. 16. (a) Langmuir isotherm of CV dye onto P powder and (b) Freundlich isotherm of CV dye onto P powder.

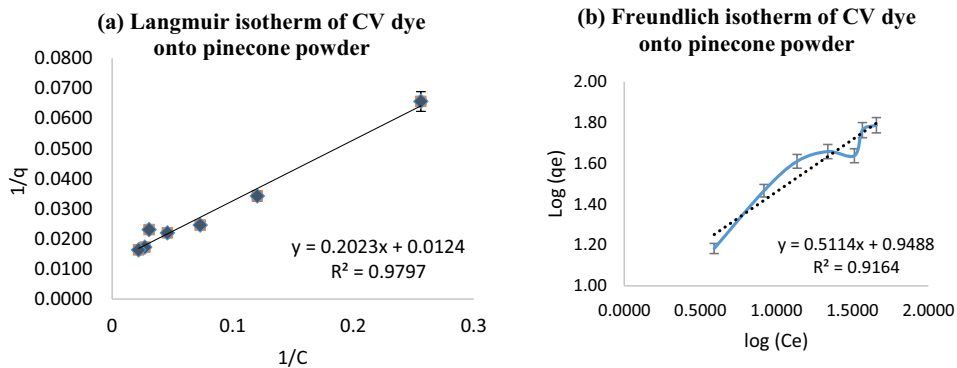


Fig. 17. (a) Langmuir isotherm of CV dye onto C powder and (b) Freundlich isotherm of CV dye onto C powder.

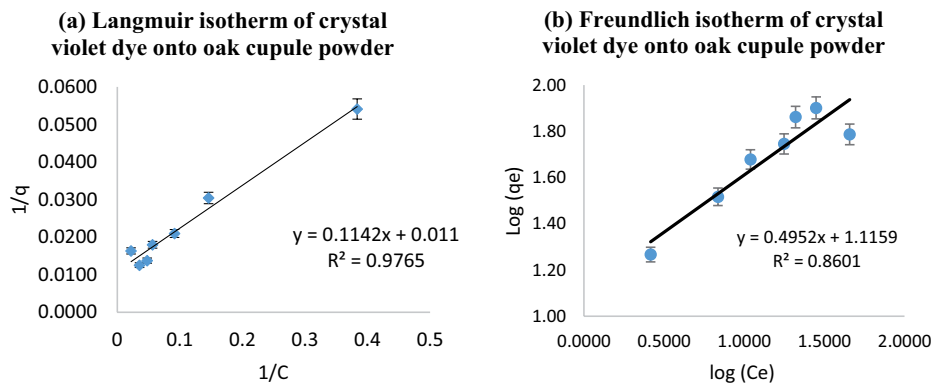


Fig. 18. (a) Langmuir isotherm of CV dye onto O powder and (b) Freundlich isotherm of CV dye onto O powder.

Langmuir and Freundlich isotherms. Table 3 summarizes the obtained results involving correlation coefficients, dimensional factors, and related constants. The R^2 values indicate that the Langmuir isotherm is the best fit for the adsorption of CV onto P, C, and O. Langmuir isotherm indicates monolayer coverage and the homogenous surface of adsorbents. For the three adsorbents, R_L values are lower than 1.0 indicating favorable adsorption of CV. The maximum adsorption capacity (q_{max}) was calculated from the intercept of the plot of the Langmuir isotherm model and found to be 80.65, 105.26, and 90.91 mg/g for P, C, and O, respectively.

3.2.8. Thermodynamics

The thermodynamic efficacy of the adsorption of CV dye onto natural adsorbent materials of P, C, and O was investigated by evaluating the thermodynamic parameters of Gibbs free energy ΔG° , enthalpy change ΔH° , and entropy ΔS° . The data obtained by plotting $\ln K_L$ vs. $1/T$ were subject for thermodynamic studies in an attempt to establish the nature of the adsorption process. The values of ΔH° (kJ/mol) and ΔS° (J/mol·K) were calculated from the slope and intercept of the plot. Table 4 shows the thermodynamic parameters

Table 3
Isotherms model constants

	Langmuir			Freundlich		
	R_L^2	R_L	K_L	R_F^2	K_f	n
Pine cone	0.9797	0.3371	0.0613	0.9164	3.2464	1.0540
Cypress fruit	0.9695	0.5228	0.0240	0.8143	4.3411	1.1473
Oak cupule	0.9765	0.2518	0.0963	0.8601	3.1275	0.8961

R_L^2 : Correlation coefficient of Langmuir isotherm; R_F^2 : Correlation coefficient of Freundlich isotherm; R_L : Dimensional factors for the Langmuir isotherm; K_f : Dimensional factors for the Freundlich isotherm; L : Langmuir constants for the adsorption; n : Freundlich constants for the adsorption.

Table 4
Thermodynamic parameters of adsorption of CV onto P, C, and O

Adsorbent	T (K)	q_m (mg/g)	Thermodynamic parameters		
			ΔG° (kJ/mol)	ΔH° (kJ/mol)	ΔS° (kJ/K·mol)
Pinecone	303	80.65	-21.27		
	313	77.45	-22.61	-27.034	0.101
	323	62.13	-26.83		
Cypress fruit	303	105.26	-33.11		
	313	99.89	-34.30	-17.168	0.090
	323	84.12	-36.63		
Oak cupule	303	90.91	-14.98		
	313	84.65	-20.34	-47.285	0.171
	323	73.23	-24.62		

of CV dye adsorption onto P, C, and O. The negative values obtained for Gibb's free energy (ΔG°) demonstrate that adsorption of CV onto P, C, and O are favorable and spontaneous. Negative values of enthalpy (ΔH°) confirm the exothermic nature of the adsorption process. Enthalpy magnitude is also indicative of the adsorption mechanism by physisorption through van der Waals if less than 20 kJ/mol or electrostatic type of forces between dye and adsorbent if it falls between 20 and 80 kJ/mol [31]. ΔH° values indicate mechanisms such as van der Waals played some part during CV uptake by P, C, and O adsorbents. The positive values obtained for entropy (ΔS°) indicate a good attraction of CV dye by P, C, and O surfaces [32].

4. Comparison with other low-cost natural biomass adsorbents

The maximum CV adsorption capacities of different natural low-cost adsorbent materials including P, C, and O were compared (Table 5). The comparison shows that P, C, and O have adsorption capacities (117.33, 85.32, and 87.39 mg/g, respectively) higher than many of the other reported adsorbents. The higher negative charge of the adsorbent surface under optimal conditions leads to an increase in the electrostatic attraction between positively charged CV species.

5. Regeneration study

The regeneration capacity of P, C, and O adsorbents decides the cost and process efficacy and plays a main role in its large application. Acetic acid is found to be the best for the regeneration of CV adsorbed [38]. 0.5 M of acetic acid was used for the elution of CV from adsorbents surfaces. Adsorption studies onto regenerated P, C, and O were carried out eight times to confirm the performance in CV removal. The adsorption percentage removal after eight cycles of regeneration is presented in Fig. 19.

After eight cycles, the surfaces of P, C, and O exhibited about 9.08%, 10.62%, and 15.95% respectively, lower adsorption capacity. This decrease in percentage removal can be ascribed to a change in surface characteristics due to repeated adsorption/desorption processes.

Table 5
Comparison of CV adsorption capacity of P, C, and O with other reported low-cost natural adsorbents

Adsorbent	q_{max} (mg/g)
Pecan nutshell (PN) [14]	94
Para chestnut husk (PCH) [14]	101
Tamarind seed [33]	18.35
Teak tree bark powder [34]	142.85
Raw tend waste [35]	42.92
Jackfruit leaf powder [36]	43.39
Pineapple leaf (<i>Ananas comosus</i>) powder [37]	158.37
Pinecone powder (present study)	80.64
Cypress fruit powder (present study)	105.26
Oak cupule powder (present study)	90.91

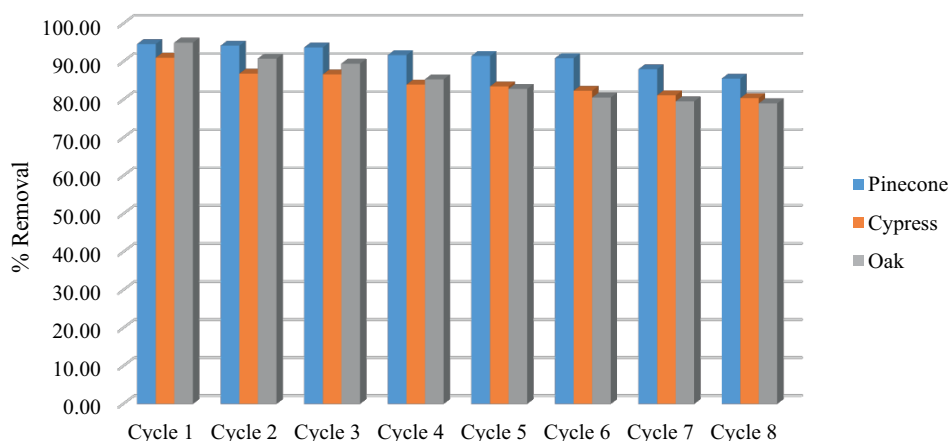


Fig. 19. Removal percentage of CV in regeneration process of P, C, and O adsorbents.

6. Conclusion

The study showed the possibility of employing powder of raw pinecone P, cypress C, and oak cupules O as adsorbents for CV dye. The experimental results show that the adsorption capacity of CV is strongly affected by the operating parameters such as contact time, pH, adsorbent dose, temperature, and initial CV concentration. Rises in initial concentration and contact time lead to an increase in the adsorption capacity of CV (mg/g). A pH of 7 is found to be the optimum for CV uptake by C adsorbent. In contrast, results showed increasing in CV uptake by P and O with increasing pH. As a comparison, 96.99%, 96.82%, and 89.85% of CV were removed by C, P, and O adsorbents, respectively, under optimized conditions. The best fit with kinetic experimental data was obtained by applying the pseudo-first-order kinetic model for C and O adsorbents, while kinetics data for P adsorbent was found to fit the pseudo-second-order. The Langmuir model fit better the adsorption results compared to the Freundlich model, with adsorption capacity of 80.64, 105.26, and 90.91 mg/g for P, C, and O, respectively. Thermodynamic studies revealed that the adsorption processes are favorable, spontaneous, and exothermic. The regeneration investigation indicates that the unmodified surfaces of P, C, and O adsorbents show good and acceptable stability.

Acknowledgment

The project was supported by Isra University, Jordan, which the authors are very grateful. Grant number: [8-38/2020/2021].

Statements and declarations

The authors declare that they have no known competing financial interests or personal relationships that could have appeared to influence the work reported in this paper.

Competing interests

The authors have no relevant financial or non-financial interests to disclose.

Author contributions

All authors contributed to the study conception and design. Material preparation, data collection and analysis were performed by all authors (Alaa Mahmoud Al-Ma'abreh, Razan Ataallah Abuasaf, Dareen A. Hmedat, Manal H. Al Khabbas, Samer Awaideh, and Gada Idrees. The first draft of the manuscript was written by Alaa Mahmoud Al-Ma'abreh and all authors commented on previous versions of the manuscript. All authors read and approved the final manuscript.

Availability of data and materials

The data that support the findings of this study are available from the corresponding author upon reasonable request.

References

- [1] A. Jahanban-Esfahlan, R. Jahanban-Esfahlan, M. Tabibiazar, L. Roufegarinejad, R. Amarowicz, Recent advances in the use of walnut (*Juglans regia* L.) shell as a valuable plant-based bio-sorbent for the removal of hazardous materials, *RSC Adv.*, 10 (2020) 7026–7047.
- [2] P. Monash, R. Niwas, G. Pugazhenth, Utilization of ball clay adsorbents for the removal of crystal violet dye from aqueous solution, *Clean Technol. Environ. Policy*, 13 (2010) 141–151.
- [3] A. Mittal, J. Mittal, A. Malviya, D. Kaur, V. Gupta, Adsorption of hazardous dye crystal violet from wastewater by waste materials, *J. Colloid Interface Sci.*, 343 (2010) 463–473.
- [4] E. Contreras, L. Sepúlveda, C. Palma, Valorization of agroindustrial wastes as biosorbent for the removal of textile dyes from aqueous solutions, *Int. J. Chem. Eng.*, (2012) 1–9, doi: 10.1155/2012/679352.
- [5] G.K. Sarma, S. Sen Gupta, K.G. Bhattacharyya, RETRACTED: adsorption of Crystal violet on raw and acid-treated montmorillonite, K10, in aqueous suspension, *J. Environ. Manage.*, 171 (2016) 1–10.
- [6] A. Adak, M. Bandyopadhyay, A. Pal, Removal of crystal violet dye from wastewater by surfactant-modified alumina, *Sep. Purif. Technol.*, 44 (2005b) 139–144.
- [7] R.S. Juang, R.C. Shiau, Metal removal from aqueous solutions using chitosan-enhanced membrane filtration, *J. Membr. Sci.*, 165 (2000) 159–167.
- [8] A. García-Sánchez, E. Álvarez-Ayuso, Sorption of Zn, Cd and Cr on calcite. Application to purification of industrial wastewaters, *Miner. Eng.*, 15 (2002) 539–547.

- [9] J.C. Moreno-Piraján, L. Giraldo, Heavy metal ions adsorption from wastewater using activated carbon from orange peel, *E-J. Chem.*, 9 (2012) 926–937.
- [10] S. Babel, Low-cost adsorbents for heavy metals uptake from contaminated water: a review, *J. Hazard. Mater.*, 97 (2003) 219–243.
- [11] M.M.R. Khan, M.W. Rahman, H.R. Ong, A.B. Ismail, C.K. Cheng, Tea dust as a potential low-cost adsorbent for the removal of crystal violet from aqueous solution, *Desal. Water Treat.*, 57 (2015) 14728–14738.
- [12] S. Bentahar, A. Dbik, M.E. Khomri, N.E. Messaoudi, A. Lacherai, Adsorption of methylene blue, crystal violet and Congo red from binary and ternary systems with natural clay: kinetic, isotherm, and thermodynamic, *J. Environ. Chem. Eng.*, 5 (2017) 5921–5932.
- [13] S. Lairini, K. El Mahtal, Y. Miyah, K. Tanji, S. Guissi, S. Boumchita, F. Zerrouq, The adsorption of Crystal violet from aqueous solution by using potato peels (*Solanum tuberosum*): equilibrium and kinetic studies, *J. Mater. Environ. Sci.*, 8 (2017) 3252–3261.
- [14] X. Pang, L. Sellaoui, D. Franco, G.L. Dotto, J. Georgin, A. Bajahzar, H. Belmabrouk, A. Ben Lamine, A. Bonilla-Petriciolet, Z. Li, Adsorption of crystal violet on biomasses from pecan nutshell, para chestnut husk, araucaria bark and palm cactus: experimental study and theoretical modeling via monolayer and double layer statistical physics models, *Chem. Eng. J.*, 378 (2019) 122101, doi: 10.1016/j.cej.2019.122101.
- [15] G. El Fawal, A. Ibrahim, M.A. Akl, Methylene blue and crystal violet dyes removal (as a binary system) from aqueous solution using local soil clay: kinetics study and equilibrium isotherms, *Egypt. J. Chem.*, 62 (2019) 541–554.
- [16] C.M. Oloo, J.M. Onyari, W.C. Wanyonyi, J.N. Wabomba, V.M. Muinde, Adsorptive removal of hazardous crystal violet dye from aqueous solution using *Rhizophora mucronata* stem-barks: equilibrium and kinetics studies, *Environ. Chem. Ecotoxicol.*, 2 (2020) 64–72.
- [17] N.S. Kumar, M. Asif, M.I. Al-Hazzaa, Adsorptive removal of phenolic compounds from aqueous solutions using pine cone biomass: kinetics and equilibrium studies, *Environ. Sci. Pollut. Res.*, 25 (2018) 21949–21960.
- [18] G.K. Cheruiyot, W.C. Wanyonyi, J.J. Kiplimo, E.N. Maina, Adsorption of toxic crystal violet dye using coffee husks: equilibrium, kinetics and thermodynamics study, *Sci. Afr.*, 5 (2019) e00116, doi: 10.1016/j.sciaf.2019.e00116.
- [19] D. Balarak, A.H. Mahvi, S. Shahbaksh, M.A. Wahab, A. Abdala, Adsorptive removal of azithromycin antibiotic from aqueous solution by *Azolla filiculoides*-based activated porous carbon, *Nanomaterials*, 11 (2021) 3281, doi: 10.3390/nano11123281.
- [20] M.B. Amar, K. Walha, V. Salvadó, Valorisation of pine cone as an efficient biosorbent for the removal of Pb(II), Cd(II), Cu(II), and Cr(VI), *Adsorpt. Sci. Technol.*, (2021) 1–12, doi: 10.1155/2021/6678530.
- [21] E. Malkoc, Y. Nuhoglu, Fixed bed studies for the sorption of chromium(VI) onto tea factory waste, *Chem. Eng. Sci.*, 61 (2006) 4363–4372.
- [22] T. Dula, K. Siraj, S.A. Kitte, Adsorption of hexavalent chromium from aqueous solution using chemically activated carbon prepared from locally available waste of bamboo (*Oxytenanthera abyssinica*), *ISRN Environ. Chem.*, (2014) 1–9, doi: 10.1155/2014/438245.
- [23] W.M. Ibrahim, Y. Abdel Aziz, S.M. Hamdy, N.S. Gad, Comparative Study for biosorption of heavy metals from synthetic wastewater by different types of marine algae, *J. Biorem. Biodegrad.*, 9 (2018) 425, doi: 10.4172/2155-6199.1000425.
- [24] A. Gholizadeh, M. Kermani, M. Gholami, M. Farzadkia, Kinetic and isotherm studies of adsorption and biosorption processes in the removal of phenolic compounds from aqueous solutions: comparative study, *J. Environ. Health Sci. Eng.*, 11 (2013), doi: 10.1186/2052-336x-11-29.
- [25] O. Abdelwahab, N. Amin, Adsorption of phenol from aqueous solutions by *Luffa cylindrica* fibers: kinetics, isotherm and thermodynamic studies, *Egypt. J. Aquat. Res.*, 39 (2013) 215–223.
- [26] R. Ahmad, Studies on adsorption of crystal violet dye from aqueous solution onto coniferous pinus bark powder (CPBP), *J. Hazard. Mater.*, 171 (2009) 767–773.
- [27] M.R. Kulkarni, T. Revanth, A. Acharya, P. Bhat, Removal of Crystal violet dye from aqueous solution using water hyacinth: equilibrium, kinetics and thermodynamics study, *Resour.-Effic. Technol.*, 3 (2017) 71–77.
- [28] A. Saeed, M. Sharif, M. Iqbal, Application potential of grapefruit peel as dye sorbent: kinetics, equilibrium and mechanism of crystal violet adsorption, *J. Hazard. Mater.*, 179 (2010) 564–572.
- [29] J. Salimi, B. Kakavandi, A.A. Babaei, A. Takdastan, N. Alavi, A. Neisi, B. Ayoubi-Feiz, Modeling and optimization of nonylphenol removal from contaminated water media using a magnetic recoverable composite by artificial neural networks, *Water Sci. Technol.*, 75 (2016) 1761–1775.
- [30] R. Lafi, I. Montasser, A. Hafiane, Adsorption of Congo red dye from aqueous solutions by prepared activated carbon with oxygen-containing functional groups and its regeneration, *Adsorpt. Sci. Technol.*, 37 (2018) 160–181.
- [31] G.R. Mahdavinia, F. Bazmizyabad, B. Seyyedi, κ -carrageenan beads as new adsorbent to remove crystal violet dye from water: adsorption kinetics and isotherm, *Desal. Water Treat.*, 53 (2015) 2529–2539.
- [32] Q. Li, Q. Yue, Y. Su, B.Y. Gao, H.J. Sun, Equilibrium, thermodynamics and process design to minimize adsorbent amount for the adsorption of acid dyes onto cationic polymer-loaded bentonite, *Chem. Eng. J.*, 158 (2010) 489–497.
- [33] H. Patel, R.T. Vashi, Adsorption of crystal violet dye onto tamarind seed powder, *E-J. Chem.*, 7 (2010) 975–984.
- [34] S. Patil, V. Deshmukh, S. Renukdas, N. Patel, Kinetics of adsorption of crystal violet from aqueous solutions using different natural materials, *Int. J. Environ. Sci.*, 1 (2011) 1116–11134.
- [35] G.K. Nagda, V.S. Ghole, Utilization of lignocellulosic waste from bidi industry for removal of dye from aqueous solution, *Int. J. Environ. Res.*, 2 (2008) 385–390.
- [36] P. Saha, S. Chakraborty, S. Chowdhury, Batch and continuous (fixed-bed column) biosorption of crystal violet by *Artocarpus heterophyllus* (jackfruit) leaf powder, *Colloids Surf., B*, 92 (2012) 262–270.
- [37] S. Neupane, S. Ramesh, R. Gandhimathi, P. Nidheesh, Pineapple leaf (*Ananas comosus*) powder as a biosorbent for the removal of crystal violet from aqueous solution, *Desal. Water Treat.*, 54 (2014) 2041–2054.
- [38] P.V. Nidheesh, R. Gandhimathi, S.T. Ramesh, T.S. Anantha Singh, Adsorption and desorption characteristics of crystal violet in bottom ash column, *J. Urban Environ. Eng.*, 6 (2012) 18–29.